AN INVESTIGATION OF THE MECHANICAL PROPERTIES OF LASER PERFORATED CFRP COMPOSITES FOR AEROSPACE APPLICATIONS

Paul Nixon[1], Martin Wood[2], Liu Yang[1] and Ross F. Minty[1]

[1]Department of Mechanical and Aerospace Engineering, University of Strathclyde Glasgow, G1 1XJ, United Kingdom
Email: paul.nixon@strath.ac.uk, Web Page: http://www.strath.ac.uk/compositematerials/
[2]CAV-Systems Ltd, No. 1, Industrial Estate, Consett, DH8 6SZ, United Kingdom

Keywords: Carbon fibre, Laser drilling, Mechanical properties, Composites, Aerospace

Abstract
Conventional wisdom would suggest an expectation that certain material properties of carbon fibre reinforced polymer (CFRP) composites would be negatively impacted by the introduction of perforations; however, initial findings have suggested this not to be the case. The present work will focus on investigating the mechanical properties of laser perforated CFRP composites by means of tensile, flexural, compressive, and short beam shear testing. The test specimens used in this investigation were manufactured from out-of-autoclave carbon fibre prepreg. A direct comparison is made between the perforated and non-perforated specimens in terms of their mechanical performance.

1. Introduction

Carbon fibre reinforced polymer (CFRP) composites have seen consistent growth in their usage as an aerospace material over the past several decades, owing to their excellent strength-to-weight ratio [1]. One example of an aerospace application for CFRP composites is in hybrid laminar flow control (HLFC) systems. This traditionally consists of a laser perforated titanium skin on aircraft leading edge surfaces. However, the effectiveness of the HLFC panel is reduced as a consequence of the additional weight of titanium in an area that would otherwise be composed of a composite material in conventional aircraft configurations, where HLFC panels are not present [2]. There is therefore a commercial interest in producing these perforated panels from light weight composite materials.

There are significant challenges to optimising the laser drilling process for effective use on composite materials due to the dissimilar thermal properties of the resin and fibres [3]. CAV-Systems Ltd specializes in laser work to provide manufacturing capability for its range of aircraft ice protection and HLFC products. This includes tailoring laser machines to suit materials such as carbon fibre by minimizing the heat affected zone (HAZ) around the hole.

The wavelength and power of a laser is selected based on the material, part geometry and rate of removal. Fibre or flashlamp pumped rod lasers can be employed to achieve this. Holes are drilled individually with typical exit hole sizes between 0.05 – 0.15 mm diameter depending on specific product requirements.

The impact of these perforations on the mechanical properties of CFRP composites remains largely unexplored in the existing literature. Most notably, a study by Young et al. [4] investigated the effect of laser drilled micro-perforations on the strength and stiffness of carbon fibre by means of tensile and compression testing. However, recent advancements in laser technology have enabled a more

comprehensive analysis to be conducted. By incorporating flexural and short beam shear testing, a deeper analysis of the effects of laser micro-perforations on the mechanical properties of CFRP composites can be achieved.

2. Experimental

2.1. Materials

The test specimens used in this investigation were manufactured from UD SkyFlex K51 Epoxy Carbon Fibre Prepreg with 33% resin content. The reinforcing fibres were Toray T700 high strength carbon fibres. The specimens incorporated fourteen layers of prepreg with a quasi-isotropic ply orientation of $[0/45/-45/90/0/45/-45]_S$ resulting in a nominal material thickness of 2 mm.

2.2. Manufacturing Test Specimens

Square panels, 2 mm thick and 300 mm wide, were manufactured in a vacuum-bagged out-of-autoclave oven curing process. The laminate, consisting of fourteen layers of prepreg with the previously mentioned ply orientation, were set upon a flat glass moulding plate. Cork tape provided a barrier around the perimeter of the laminate as a means of edge control that helped maintain the shape of the laminate during cure and prevented any resin leakage. Release film was applied to the surface of the laminate and a flat aluminium plate was positioned atop to provide an even pressure distribution during the curing process. Breather fabric was placed over the setup to allow airflow throughout the vacuum bag and to bleed any excess resin. The setup was inserted into an enveloped vacuum bag, through which a vacuum port was connected to the curing oven vacuum pump. The laminate was cured under vacuum pressure at 125°C, with an initial ramp from room temperature at 2°C/minute. Once cooled, the test specimens were water jet cut from the CFRP panel.

2.3. Laser Perforation

The specimens were sent to CAV-Systems where they were laser perforated. The laser perforation process was designed to create a square array of holes with a 1.5 mm hole pitch. Due to the differing widths of each test specimen type, the total number of holes varied across the different tests. It was also ensured that holes were drilled no closer than 0.5 mm from the edge of the test specimens to avoid creating notches that may induce stress concentrations during loading that could lead to premature failure [1]. The laser perforated test specimens are illustrated in Figure 1.

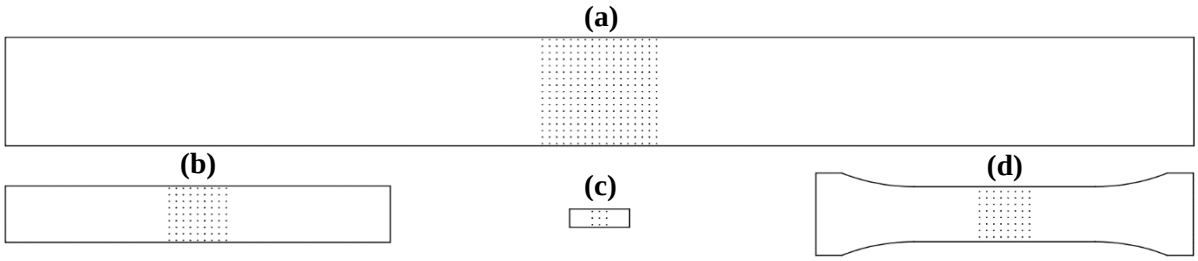

Figure 1. Test specimens with perforated gauge section: (a) Tensile, (b) Flexural, (c) Short beam shear, (d) Compression.

2.4. Optical Microscopy

In order to inspect the hole geometry and quality, and to assess the extent of laser induced damage on the test specimens, micrographs of the entry and exit holes were taken. Transmitted light microscopy was employed to accurately determine the hole diameters as this allowed light to pass through the hole, providing a clearer definition of the hole edges. Image processing software was then used to measure the hole diameters. It was found that the mean hole entrance and exit diameters were 64.9 μm and 48.9

µm, respectively. This corresponds to a hole taper ratio of 1.33 which is relatively small compared to previous studies involving laser micro-drilled holes [5,6]. The reason for this taper can be attributed to several factors. One such factor is that at deeper hole depths a larger proportion of the laser energy is absorbed by the sidewall surfaces, leading to a reduction in the available laser energy at the hole exit, and hence a reduction in the hole exit diameter [7].

It was observed through reflected light microscopy that the HAZ, although relatively small, is larger around the entry holes than the exit holes. It was also observed that the HAZ exhibits an elliptical geometry. This is due to the anisotropic thermal conductivity within the composite material, where heat is conducted extremely well along the fibre direction, but less effectively through the resin matrix [5].

2.5. Mechanical Testing

Due to there currently being no recognised standard for testing composite materials with micro-drilled holes [8], existing ASTM standards were adapted to suit the requirements of this unique type of specimen. Four mechanical testing methods were used to evaluate the effect that laser perforation had on the mechanical properties of the material under investigation. All tests were performed using a Testometric X500 Universal Testing Machine with a 50 kN load cell.

Tensile tests were conducted according to ASTM D3039 [9], with test specimen dimensions of 25 x 250 mm. Aluminium end tabs of thickness 1.5 mm were applied to the specimens using Permabond ET538 two-part epoxy. The bonded tab length was calculated from the following equation (Eq. 1).

$$L_{min} = F^{tu}h/2F^{su} \quad (1)$$

Where L_{min} is the minimum required tab length (mm), F^{tu} is the ultimate tensile strength of the test material (MPa), h is the test material thickness (mm), and F^{su} is the ultimate shear strength of the adhesive (MPa). A tab length of 40 mm was determined to be suitable for effective load transfer during tensile testing.

Flexural tests were performed by means of a three-point bending test based on ASTM D7264 [10], with test specimen dimensions of 13 x 81 mm and support span length of 67 mm. Specimens were loaded until failure occurred on either one of its outer surfaces, either by tensile cracking or local buckling.

To determine the compressive strength and modulus, the modified ASTM D695 [11] method was adopted, utilising an anti-buckling compression rig to prevent failure by Euler buckling. G10 epoxy glass fibre end tabs were bonded to the specimens to increase the area subjected to end loading and prevent premature failure due to end crushing, thereby promoting compressive failure within the gauge length. Test specimens were dog bone shaped, with a 12.7 mm wide, 16 mm long gauge length, which is defined as the distance between the end tabs. The 16 mm gauge length was chosen to accommodate the 10 mm perforated section, with 3 mm allowance on either side to mitigate the induced stress concentration effect from the tab ends.

To assess the effect of the perforations on the shear properties of the material, short beam shear tests were conducted following ASTM D2344 [12] guidelines. Specimens of width 4.2 mm with a support span length of 10 mm were loaded until there was a load drop-off of 30 % from the peak load. Microscopy analysis was used to confirm that the failure mode was by midplane interlaminar shear.

3. Results and Discussion

3.1. Tensile Tests

Presented in Figure 2 are the values of the ultimate tensile strength and tensile modulus for each of the perforated and non-perforated test specimens. Tensile specimens were loaded at a constant crosshead speed of 2 mm/min until failure. Strain measurements were taken using a 50 mm gauge length extensometer, and the tensile chord modulus was calculated between strain values of 0.1 % and 0.3 %. The extensometer was removed prior to failure to prevent it from being damaged by the explosive failure mechanism.

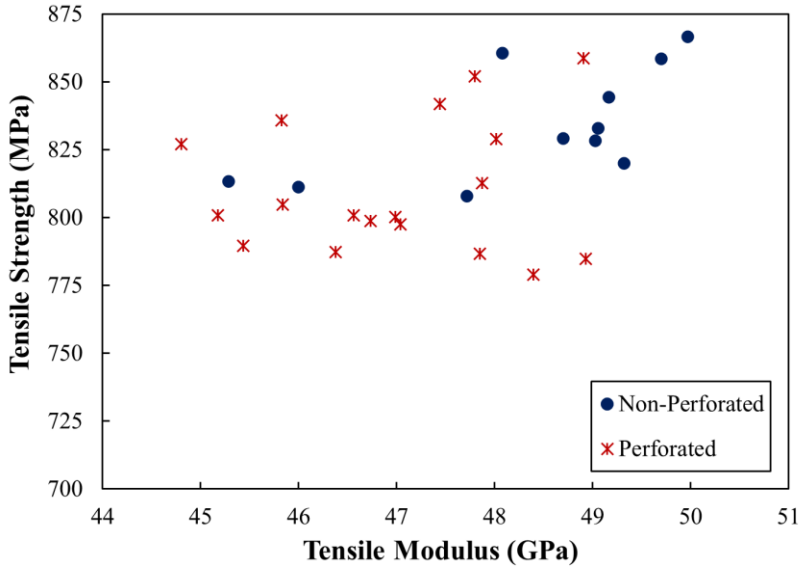

Figure 2. Ultimate tensile strength and tensile modulus of perforated and non-perforated specimens.

Figure 3 displays a comparison of the mean values for tensile strength and tensile modulus between the perforated and non-perforated tests and the standard error associated with these results.

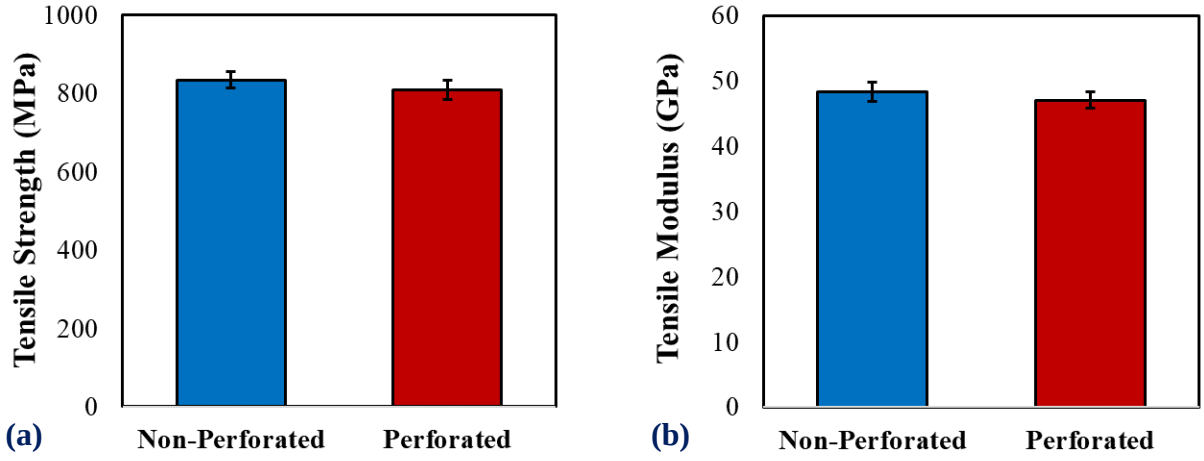

Figure 3. Comparison of tensile properties in non-perforated and perforated CFRP composites: (a) Tensile strength, (b) Tensile modulus.

Both the tensile strength and tensile modulus of the perforated specimens were found to be 97.2 % of that of the non-perforated specimens. The mean tensile strength of the non-perforated specimens was 834.1 MPa with a coefficient of variation (CV) of 2.5 %, whilst that of the perforated specimens was

810.5 MPa with a CV of 3.0 %. The mean tensile modulus of the non-perforated specimens was 48.4 GPa with a CV of 3.1 %, compared to 47.0 GPa with a CV of 2.7 % for the perforated specimens.

Failure mechanisms in both the perforated and non-perforated tensile specimens were similar, with both sets of tests exhibiting explosive failure in the centre of the gauge section. Figure 4 shows images of the failed test specimens that are representative of the typical failure mode observed across all tests.

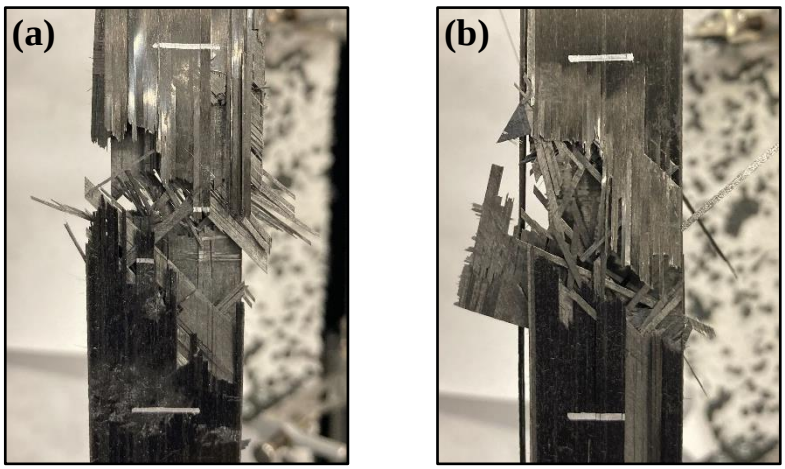

Figure 4. Failed tensile specimens: (a) Non-perforated, (b) Perforated.

3.2. Flexural Tests

The flexural test results are illustrated in Figure 5 by force-deflection plots, displaying mean values of peak force and the corresponding coefficient of variation in the results. Specimens were loaded at a constant crosshead speed of 1 mm/min until failure occurred, which was indicated by a significant drop-off in force. Force and displacement measurements were made using the integrated load cell and by tracking crosshead displacement during loading.

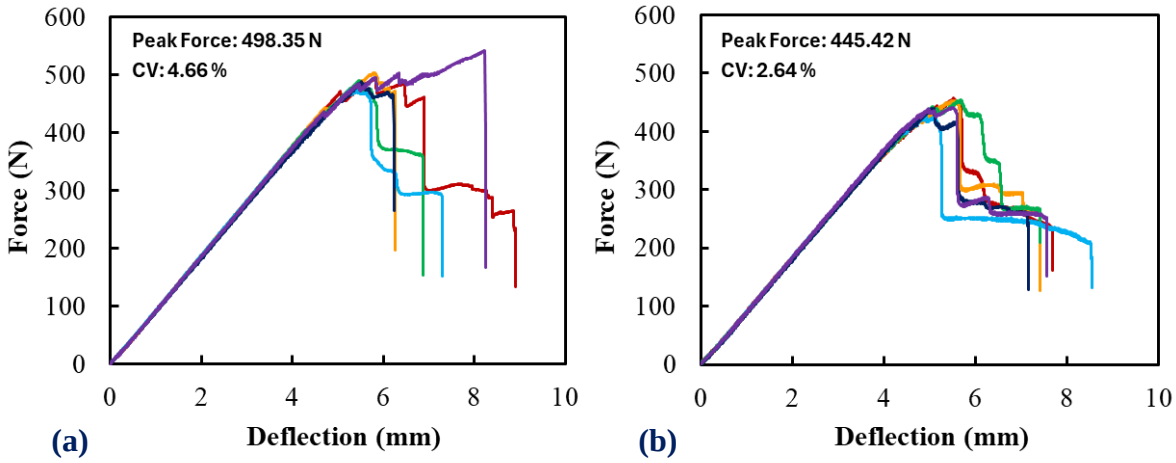

Figure 5. Three-point bending force-deflection curves for non-perforated (a) and perforated (b) CFRP specimens.

Across all flexural tests, the perforated specimens consistently exhibited a lower peak force than their non-perforated counterparts, with a 10.6 % lower mean peak force. One possible reason for this could be that the perforations may act as initiation points for surface damage when in contact with the loading

nose, leading to premature failure of the perforated specimens. Values for the bending strength and modulus are presented in Table 1, where it can be seen that the mean bending modulus of the perforated specimens was 3.7 % lower than that of the non-perforated specimens.

Table 1. Bending strength and modulus for non-perforated and perforated CFRP specimens.

Specimen Type	Bending Strength MPa (CV %)	Bending Modulus GPa (CV %)
Non-Perforated	904.92 (5.02)	62.07 (0.52)
Perforated	802.51 (2.97)	59.76 (0.74)

It is proposed that for future testing of specimens with a centrally perforated gauge section, a four-point bending configuration should be used as this would ensure that the perforated area is not in direct contact with the loading nose.

3.3. Short Beam Shear Tests

In order to characterise the effect of laser perforation on the interlaminar shear strength (ILSS) of the CFRP specimens, short beam shear (SBS) tests were carried out. Specimens were loaded at 1 mm/min until failure, defined by a 30 % drop in load. Once it was confirmed through microscopy analysis that all the specimens failed by midplane interlaminar shear, SBS strength was calculated for each specimen from Eq. 2.

$$F^{sbs} = \frac{3}{4} \times \frac{P_m}{b \times h} \tag{2}$$

Where F^{sbs} is the short beam shear strength (MPa), P_m is the maximum load during the test (N), b is the specimen width (mm), and h is the specimen thickness (mm). The results from these tests are presented in Figure 6 by force deflection plots, with the mean values of SBS strength and corresponding coefficient of variation displayed.

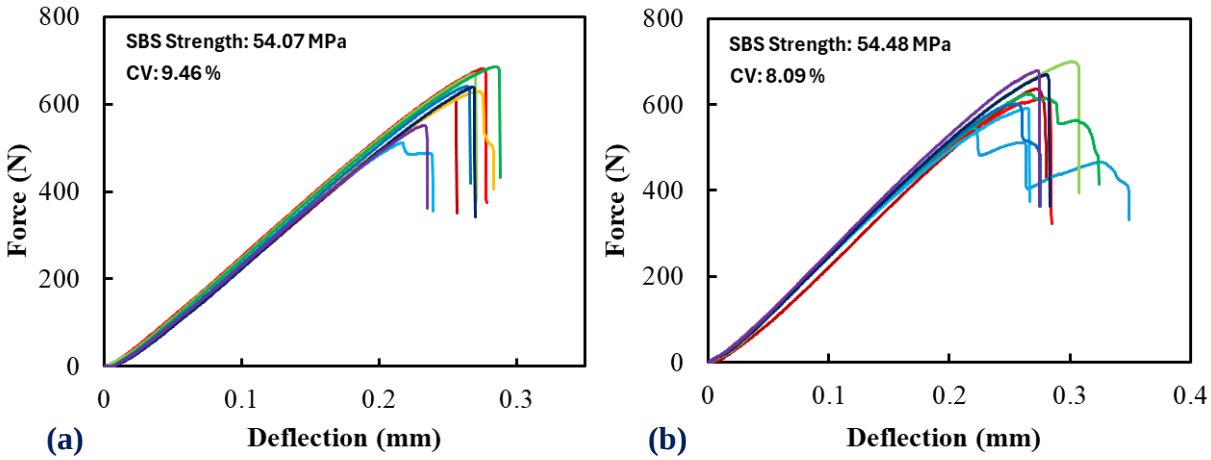

Figure 6. Short beam shear force-deflection curves for non-perforated (a) and perforated (b) CFRP specimens.

The results indicate that the laser perforation process had no discernable effect on the short beam shear strength of the CFRP specimens. This is evidenced by comparable mean values, with both sets of tests

showing similar variation in results. Future work should aim to determine the threshold of perforation at which a measurable effect on the short beam shear strength becomes evident.

3.4. Compression Tests

The results from compression testing are detailed in Table 2, with Figure 7 displaying the average compressive strengths of the perforated and non-perforated sets of tests. The tests were conducted with a constant crosshead speed of 1.3 mm/min and were terminated once the specimen failed within the gauge length with an acceptable failure mode.

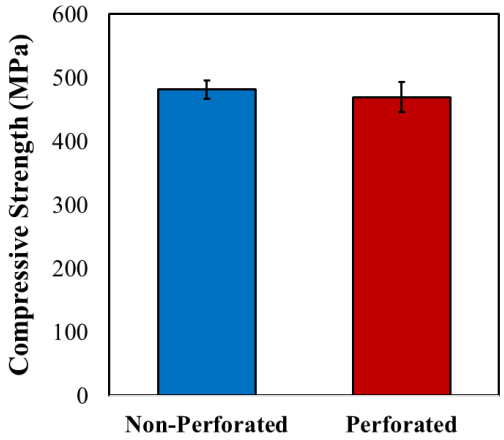

Figure 7. Comparison of compressive strength of non-perforated and perforated CFRP composites.

The perforated specimens exhibited 97.5 % of the compressive strength of the non-perforated specimens, showing a significantly higher retention of compressive strength than has been previously reported [4]. There was also no observable difference in compressive modulus, suggesting that the laser perforation process has minimal impact on the compressive properties of the CFRP specimens.

Table 2. Compressive strength and modulus for non-perforated and perforated CFRP specimens.

Specimen Type	Compressive Strength MPa (CV %)	Compressive Modulus GPa (CV %)
Non-Perforated	481.27 (2.93)	39.12 (6.01)
Perforated	469.46 (5.03)	39.10 (13.18)

4. Conclusions

In this work, four mechanical testing methods were employed to characterise the effects of laser perforation on the mechanical properties of CFRP composites. It was found that both the tensile strength and tensile modulus were reduced by only 2.8 %. The results suggest that the laser perforation process does not have a detrimental impact on the strength and stiffness of the CFRP composite, indicating its potential viability for use in aerospace applications. The results from flexural testing showed that the peak load supported by the perforated specimens was 10.6 % lower than that of the non-perforated specimens, a considerably larger reduction than was found in tensile testing. One possible explanation for this is that surface damage arises from the contact between the loading nose and test specimen surface, with perforations potentially amplifying this effect by serving as points of initiation for surface damage, contributing to the premature failure of the specimen. In terms of the interlaminar shear

properties of the CFRP specimens investigated, the results from short beam shear testing revealed that there was no apparent effect on the short beam shear strength of the laser perforated composites. Results from compression testing showed a marginal decrease of 2.5 % in compressive strength as a result of laser perforation, with there being no detectable effect on the compressive modulus.

Acknowledgments
The authors would like to gratefully acknowledge CAV-Systems Ltd. for their support of this research.

References

[1] K.F. Tamrin, N.A. Sheikh, S.M. Sapuan. Laser drilling of composite material: A review. In *Hole-Making and Drilling Technology for Composites*. Woodhead Publishing, 2019.
[2] T. Young, B. Mahony, B. Humphreys, E. Totland, A. McClafferty, J. Corish. Durability of hybrid laminar flow control (HLFC) surfaces. *Aerospace Science and Technology*, Volume 7, Issue 3: 181-190, 2003.
[3] Z.L. Li, H.Y. Zheng, G.C. Lim, P.L. Chu, L. Li. Study on UV laser machining quality of carbon fibre reinforced composites. *Composites Part A: Applied Science and Manufacturing*, Volume 41, Issue 10: 1403-1408, 2010.
[4] T. Young, D. O'Driscoll. Impact of Nd-YAG laser drilled holes on the strength and stiffness of laminar flow carbon fibre reinforced composite panels. *Composites Part A: Applied Science and Manufacturing*, Volume 33, Issue 1: 1-9, 2002.
[5] W.S.O. Rodden, S.S. Kudesia, D.P. Hand, J.D.C. Jones. A comprehensive study of the long pulse Nd:YAG laser drilling of multi-layer carbon fibre composites. *Optics Communications*, Volume 210, Issues 3–6: 319-328, 2002.
[6] T.M. Young. Impact of Nd-YAG Laser Drilling on the Fatigue Characteristics of APC-2A/AS4 Thermoplastic Composite Material. *Journal of Thermoplastic Composite Materials*, Volume 21, Issue 6: 543-555, 2008.
[7] F.A. Al-Sulaiman, B.S. Yilbas, M. Ahsan. CO2 laser cutting of a carbon/carbon multi-lamelled plain-weave structure. *Journal of Materials Processing Technology*, Volume 173, Issue 3: 345-351, 2006.
[8] N. Geier, K. Patra, R.S. Anand, S. Ashworth, B.Z. Balázs, T. Lukács, G. Magyar, P. Tamás-Bényei, J. Xu, J.P. Davim. A critical review on mechanical micro-drilling of glass and carbon fibre reinforced polymer (GFRP and CFRP) composites. *Composites Part B: Engineering*, Volume 254, 2023.
[9] ASTM Committee D30. D3039/D3039M-17: Standard Test Method for Tensile Properties of Polymer Matrix Composite Materials. *Annual Book of ASTM Standards*, Volume 15, 2017.
[10] ASTM Committee D30. D7264/D7264M-21: Standard Test Method for Flexural Properties of Polymer Matrix Composite Materials. *Annual Book of ASTM Standards*, Volume 15, 2021.
[11] ASTM Committee D20. D695-23: Standard Test Method for Compressive Properties of Rigid Plastics. *Annual Book of ASTM Standards*, Volume 8, 2021.
[12] ASTM Committee D30. D2344/D2344M-22: Standard Test Method for Short-Beam Strength of Polymer Matrix Composite Materials and Their Laminates. *Annual Book of ASTM Standards*, Volume 15, 2022.